A double-spike method for K–Ar measurement: A technique for high precision in situ dating on Mars and other planetary surfaces

K.A. Farley [a,*], J.A. Hurowitz [b], P.D. Asimow [a], N.S. Jacobson [c], J.A. Cartwright [a]

[a] *Division of Geological and Planetary Sciences, Caltech, Pasadena, CA 91125, USA*
[b] *Jet Propulsion Laboratory, Caltech, Pasadena, CA 91109, USA*
[c] *NASA Glenn Research Center, Cleveland, OH 44135, USA*

Abstract

A new method for K–Ar dating using a double isotope dilution technique is proposed and demonstrated. The method is designed to eliminate known difficulties facing in situ dating on planetary surfaces, especially instrument complexity and power availability. It may also have applicability in some terrestrial dating applications. Key to the method is the use of a solid tracer spike enriched in both ^{39}Ar and ^{41}K. When mixed with lithium borate flux in a Knudsen effusion cell, this tracer spike and a sample to be dated can be successfully fused and degassed of Ar at <1000 °C. The evolved $^{40}Ar^*/^{39}Ar$ ratio can be measured to high precision using noble gas mass spectrometry. After argon measurement the sample melt is heated to a slightly higher temperature (∼1030 °C) to volatilize potassium, and the evolved $^{39}K/^{41}K$ ratio measured by Knudsen effusion mass spectrometry. Combined with the known composition of the tracer spike, these two ratios define the K–Ar age using a single sample aliquot and without the need for extreme temperature or a mass determination. In principle the method can be implemented using a single mass spectrometer.

Experiments indicate that quantitative extraction of argon from a basalt sample occurs at a sufficiently low temperature that potassium loss in this step is unimportant. Similarly, potassium isotope ratios measured in the Knudsen apparatus indicate good sample-spike equilibration and acceptably small isotopic fractionation. When applied to a flood basalt from the Viluy Traps, Siberia, a K–Ar age of 351 ± 19 Ma was obtained, a result within 1% of the independently known age. For practical reasons this measurement was made on two separate mass spectrometers, but a scheme for combining the measurements in a single analytical instrument is described. Because both parent and daughter are determined by isotope dilution, the precision on K–Ar ages obtained by the double isotope dilution method should routinely approach that of a pair of isotope ratio determinations, likely better than ±5%.

1. INTRODUCTION

Absolute ages are critical for deciphering the timing, rates, and in many cases, the identity of processes that shape planetary surfaces. As a consequence the development of accurate surface chronologies is an important step in elucidating the evolution of terrestrial bodies in the Solar System. This is especially true for Mars, which carries a long and rich geologic record documented with spectacular resolution by numerous orbiting and landed missions (e.g., Kieffer et al., 1992; Bell, 2008; Carr and Head, 2010). For example, surface morphology, mineralogy, and lithology provide evidence for dramatic climate change on Mars, with obvious implications for habitability (e.g., Carr, 1996; Bibring et al., 2006; Murchie et al., 2009; Ehlmann et al., 2011). However in the absence of sample return or

---

* Corresponding author.
E-mail address: farley@gps.caltech.edu (K.A. Farley).

in situ dating measurements, we have no absolute markers that can be used to calibrate the planet's increasingly well-documented surface chronology. A technique to accurately measure ages from a few select locations within the established relative stratigraphy of Mars would be transformative, enabling placement of direct quantitative constraints on the timing and rates of impact, volcanic, sedimentary, climatic, and aqueous processes on the martian surface. This work proposes and implements a new methodology with the potential to provide such age determinations. The method is capable of accuracy and precision of ages of better than 5%, and is amenable to space-flight application.

Impact craters are a dominant feature on Mars, and one approach for establishing absolute ages on the surface is through statistical methods calibrated to radiometric ages and abundances of craters on the Moon. This technique was used to date distinct regions of Mars, leading to the identification of three epochs: Noachian (4.57–3.7 Ga), Hesperian (3.7–3.3/2.9 Ga) and Amazonian (3.3/2.9 Ga – present) (Hartmann and Neukum, 2001). While progress has been made improving the precision of such ages (e.g., Hauber et al., 2011), precision is not equivalent to accuracy. There are two inescapable issues regarding the application of crater counting techniques to Mars: (1) "Any estimate of the martian absolute chronology involves, implicitly or explicitly, an estimate of the Mars/Moon cratering rate ratio" (Hartmann and Neukum, 2001); and (2) Compared to the moon, Mars is geologically active, continually removing the record of craters and therefore causing bias towards younger ages. As a result, uncertainties in absolute ages derived from crater counting are fairly large, exceeding a factor of two in portions of martian geologic history where constraints on crater flux are particularly poor. These issues will continue to cast doubt on dates obtained by the method until independent age tie-points are provided for Mars.

A number of radiometric dating techniques have been and continue to be investigated for in situ application on other planets, most notably based on the rubidium-strontium (Anderson et al., 2012) and potassium-argon (Swindle, 2001; Swindle et al., 2003; Talboys et al., 2009; Cho et al., 2012; Cohen, 2012) methods. Since the present work involves the K–Ar method, we focus exclusively on this technique. K–Ar dating is based on the branched decay of ^{40}K to ^{40}Ar. With a ^{40}K half-life of 1.249 Gyr (Renne et al., 2010), the chronometer is applicable across the entire span of geologic time. K–Ar dating was among the earliest radiometric chronometers to be developed, and its application to basalts was critical to the confirmation of plate tectonics and the development of the magnetic polarity timescale. The K–Ar method is now most often implemented using the ^{40}Ar–^{39}Ar variant, in part because the ^{40}Ar–^{39}Ar method requires a single mass spectrometer and analysis of a single sample aliquot (e.g., McDougall and Harrison, 1988).

The development of the conventional K–Ar method early in the history of isotope geochemistry arose from several factors that also make it attractive for in situ dating. Because potassium is typically a major element in potential dating targets (especially basalts), there are many techniques available for determining the abundance of the parent isotope. These include X-ray spectroscopy and laser-induced breakdown spectroscopy, both of which have been undertaken on the surface of Mars (Gellert et al., 2006; Maurice et al., 2012). In addition, the effects of ingrowth on the abundance of ^{40}Ar tend to be very large and as a consequence relatively low Ar sensitivity and percent level precision on Ar isotopic ratios are adequate for many dating applications. Such levels have been achieved on Mars (Mahaffy et al., 2012).

The K–Ar method has several notable drawbacks for in situ dating (e.g., Bogard, 2009). In the conventional implementation of the method, Ar is released from an aliquot by vacuum fusion. This creates two important complications. First, the amount of power required to heat the sample to fusion (often >1200 °C) may be prohibitive on a spacecraft. Second, combining a K concentration with the Ar amount obtained by fusion requires a technique to accurately estimate the aliquot mass. Thus a conventional approach requires the complexity of at least three separate analytical instruments. Bogard (2009) describes an additional complication involving the interpretation (rather than the measurement) of K–Ar ages, an issue we consider in the discussion section.

The method proposed here requires neither high fusion temperatures, nor a mass measurement to relate potassium and argon to each other. It permits potassium and argon measurement on a single sample aliquot using a single analytical instrument. The technique takes advantage of flux digestion of the target sample to surmount the issue of high fusion temperatures. It employs double isotope dilution using a tracer containing known quantities of the rare isotopes ^{41}K and ^{39}Ar to eliminate the need for a mass determination and to permit the age to be calculated exclusively from isotope ratios. We suggest this methodology is sufficiently simple, practical, and precise to be useful in terrestrial laboratories, and provides a straightforward path towards implementation of a high precision in situ geochronology capability on planetary surfaces.

1.1. The double isotope dilution scheme

The age equation for the K–Ar system is:

$$t = \frac{1}{\lambda} \ln \left(\frac{\lambda}{\lambda_e} \frac{^{40}\text{Ar}^*}{^{40}\text{K}} + 1 \right) \qquad (1)$$

where λ is the total ^{40}K decay constant, λ_e is the decay constant for the electron capture decay mode that produces ^{40}Ar, t is the K–Ar age, and ^{40}K and ^{40}Ar* are abundances in atomic units. ^{40}Ar* is the ^{40}Ar abundance attributable to in situ radioactive decay. Thus a K–Ar age determination requires measurement of the ^{40}Ar*/^{40}K ratio.

Potassium consists of three isotopes: ^{39}K (93.3%), ^{40}K (0.0117%), and ^{41}K (6.73%). For isotope dilution ^{40}K measurements, ^{41}K of high isotopic purity (>99%) is readily available. There are three stable isotopes of argon (^{36}Ar, ^{38}Ar, and ^{40}Ar) and isotope dilution is usually done using ^{38}Ar as a tracer. Since ^{38}Ar is a useful indicator of cosmic ray exposure of potentially analyzed materials, we consider instead the use of synthetic ^{39}Ar. This radioactive isotope

has a half-life of 269 years and is routinely produced by neutron irradiation of ^{39}K-bearing substances. Depending on reactor conditions, ^{40}Ar/^{39}Ar ratios ≪1% can be obtained without significant production of either ^{36}Ar or ^{38}Ar (McDougall and Harrison, 1988).

As described below, our method requires enriched ^{41}K and ^{39}Ar tracer spike in a single material. To accomplish this goal, we prepared a synthetic silicate, hereafter referred to as the spike glass, with ~7 wt% K_2O consisting of highly enriched ^{41}K (see next section for details). The glass was then neutron irradiated to produce ^{39}Ar from the small amount of ^{39}K present. Because the glass is essentially free of Cl and Ca, production of Ar isotopes from these elements is negligible. For the double isotope dilution technique, a sample to be dated is combined with an aliquot of the spike glass, and fused to release and measure argon and potassium isotopes. The ^{40}Ar*/^{40}K ratio required for an age measurement is determined as follows (definitions of variables are provided in Table 1).

First, for Ar:

$$^{40}\text{Ar}_m = {}^{40}\text{Ar}^* + {}^{40}\text{Ar}_{air} + {}^{40}\text{Ar}_{spk} \tag{2}$$

$$^{36}\text{Ar}_m = {}^{36}\text{Ar}_{air} \tag{3}$$

$$^{39}\text{Ar}_m = {}^{39}\text{Ar}_{spk} \tag{4}$$

where subscripts m, air, and spk refer to measured, air-derived, and spike amounts. Eq. (2) is the mass balance for ^{40}Ar and indicates that some of the ^{40}Ar is derived from "contamination" with atmospheric argon (in the present case from terrestrial air, but martian atmosphere in the case of a Mars rover application) and some is reactor-produced in the spike. Eq. (4) indicates that all ^{39}Ar is spike-derived. Here we are assuming that there is no cosmogenic ^{36}Ar in the sample, such that atmosphere is the only source of this isotope (Eq. (3)); in a system with substantial cosmic ray

exposure, ^{38}Ar could be used to quantify and correct for cosmogenic ^{36}Ar.

Combining Eqs. (2)–(4) yields:

$$^{40}\text{Ar}^* = \left(R_m - \left(\frac{^{40}\text{Ar}}{^{36}\text{Ar}}\right)_{air} \left(\frac{^{36}\text{Ar}}{^{39}\text{Ar}}\right)_m - R_{spk} \right) {}^{39}\text{Ar}_{spk} \tag{5}$$

where R_m is the measured ^{40}Ar/^{39}Ar ratio of the sample-spike mixture, (^{40}Ar/^{36}Ar)$_{air}$ is the atmospheric Ar isotope ratio, and R_{spk} is the known ^{40}Ar/^{39}Ar ratio of the spike glass.

In the case of potassium:

$$^{39}\text{K}_m = {}^{39}\text{K}_u + {}^{39}\text{K}_{spk} \tag{6}$$

$$^{41}\text{K}_m = {}^{41}\text{K}_u + {}^{41}\text{K}_{spk} \tag{7}$$

$$^{39}\text{K}_u = r_{40}\,{}^{39}\text{K}_u \tag{8}$$

where u refers to the unknown sample and the remaining subscripts are as defined above. Eqs. (6) and (7) simply reflect mass balance. Eq. (8) states that the isotopic composition of the unknown sample is that of natural (terrestrial) potassium ($r_{40} = (^{40}$K/^{39}K)$_{nat}$) and is useful because it permits measurement of the parent isotope via the most abundant isotope of potassium. Work on many different types of samples, including martian meteorites, lunar rocks, and chondrites, confirms extremely limited (<1%) isotopic variability of potassium in the solar system (Humayun and Clayton, 1995), and supports the generality of the terrestrial isotope composition we assume.

Combining Eqs. (6)–(8) and defining the additional ratios $r_{spk} = (^{39}$K/^{41}K)$_{spk}$, $r_m = (^{39}$K/^{41}K)$_m$ and $r_{nat} = (^{39}$K/^{41}K)$_{nat}$ yields:

$$^{39}\text{K}_u = r_{40}\left(\frac{r_{spk} - r_m}{\frac{r_m}{r_{nat}} - 1} \right) {}^{41}K_{spk} \tag{9}$$

Combining Eqs. (5) and (9) yields the ratio from which the K–Ar age is determined:

$$\frac{^{40}\text{Ar}^*}{^{40}\text{K}} = \frac{\left(R_m - \left(\frac{^{40}\text{Ar}}{^{36}\text{Ar}}\right)_{air} \left(\frac{^{36}\text{Ar}}{^{39}\text{Ar}}\right)_m - R_{spk} \right)}{r_{40}\left(\frac{r_{spk}-r_m}{\frac{r_m}{r_{nat}}-1}\right)} \left(\frac{^{39}\text{Ar}}{^{41}\text{K}}\right)_{spk} \tag{10}$$

Note that Eq. (10) shows that the K–Ar age can be computed directly from measured isotopic ratios without knowledge of the mass of the sample or of the spike glass. This works because the ratio (^{39}Ar/^{41}K)$_{spk}$ is known independently and is fixed.

As written, Eq. (10) effectively requires two concentration determinations be made on the spike glass to obtain (^{39}Ar/^{41}K)$_{spk}$, one of ^{39}Ar and one of ^{41}K. An alternative approach, not implemented here, can eliminate this requirement. It is common practice in ^{40}Ar–^{39}Ar geochronology to use an age standard to eliminate variables that are difficult to constrain independently, especially the efficiency with which ^{39}K is transmuted to ^{39}Ar in the nuclear reactor. A similar approach could be used to eliminate the need to directly measure the spike ratio (^{39}Ar/^{41}K)$_{spk}$. Eq. (10) can be rewritten:

$$\frac{^{40}\text{Ar}^*}{^{40}\text{K}} = f(sample)\left(\frac{^{39}\text{Ar}}{^{41}\text{K}}\right)_{spk} \tag{11}$$

Table 1
Definition of variables.

$^{40}\text{Ar}^*$	In situ radiogenic Ar amount in unknown
$^{39}\text{Ar}_{spk}$, $^{40}\text{Ar}_{spk}$	Amounts of Ar in spike glass
$^{40}\text{Ar}_m$, $^{36}\text{Ar}_m$, $^{39}\text{Ar}_m$	Amounts of Ar in unknown
$^{40}\text{Ar}_{air}$, $^{36}\text{Ar}_{air}$	Air-derived Ar amounts in unknown
$(^{40}\text{Ar}/^{36}\text{Ar})_{air}$	Known atmospheric argon isotope ratio
$R_{spk} = (^{40}\text{Ar}/^{39}\text{Ar})_{spk}$	Independently determined spike composition
$R_m = (^{40}\text{Ar}/^{39}\text{Ar})_m$	Measured on unknown
$^{39}\text{K}_u$, $^{40}\text{K}_u$, $^{41}\text{K}_u$	Amounts of K in unknown
$^{39}\text{K}_{spk}$, $^{41}\text{K}_{spk}$	Amounts of K in spike glass
$r_m = (^{39}\text{K}/^{41}\text{K})_m$	Measured on unknown
$r_{spk} = (^{39}\text{K}/^{41}\text{K})_{spk}$	Independently determined spike composition
$r_{nat} = (^{39}\text{K}/^{41}\text{K})_{nat}$	Natural K isotopic composition (known)
$r_{40} = (^{40}\text{K}/^{39}\text{K})_{nat}$	Natural K isotopic composition (known)
J_{ID}	Calibration parameter, Eq. (13)
t_{std}	Independently known age of standard
t	K–Ar age of unknown
$f(sample)$	A function of measured quantities, Eqs. (10), (11)

where $f(sample)$ is a function of measured quantities on a sample as well as known properties of the isotopic composition of K and Ar (compare with Eq. (10) for exact definition of $f(sample)$). Combining Eq. (11) with the age Eq. (1) gives:

$$t = \frac{1}{\lambda} \ln \left(\frac{\lambda}{\lambda_e} \left(\frac{^{39}Ar}{^{41}K} \right)_{spk} f(sample) + 1 \right) \qquad (12)$$

By analogy to the ^{40}Ar–^{39}Ar approach, we can define the isotope dilution "calibration parameter", J_{ID}, that combines the first two terms in the natural logarithm. Analyzing an age standard with known age t_{std} and rearranging Eq. (12) yields:

$$J_{ID} = \frac{e^{\lambda t_{std}} - 1}{f(standard)} \frac{\lambda}{\lambda_e} \qquad (13)$$

And thus:

$$t = \frac{1}{\lambda} \ln(J_{ID} f(sample) + 1) \qquad (14)$$

This is the age equation for the double isotope dilution method using an age standard calibration. Using this form would eliminate the need to determine absolute concentrations even on the spike glass – all required measurements are isotopic ratios. Further work is necessary to evaluate the merits of this age-standard approach relative to standard laboratory measurements of the spike composition.

2. IMPLEMENTATION

A particular attraction to the method outlined above is that, by suitable preparation, a single mass spectrometer can be used for the entire age determination. The method can be implemented as follows. Both sample and spike glass are introduced into a Knudsen cell – a small Mo container with a carefully machined orifice in the lid (Fig. 1). The weights of spike glass and sample need not be measured, though as in any isotope dilution method the relative amounts of spike and sample isotopes need to provide a measurable contrast with natural isotopic compositions of the elements being analyzed. For our current implementation, we use ∼10 mg of sample and ∼150 μg of spike glass. The crucible is preloaded with ∼150 mg of degassed 50:50 lithium metaborate:lithium tetraborate (hereafter "lithium borate"). The flux serves to lower the melting point of the system to ∼850 °C, and furthermore, it enhances the likelihood of equilibration of spike and sample isotopes (especially of potassium) during heating. Incomplete equilibration of isotopes could lead to inaccurate bulk isotopic ratio measurements, and is of special concern because spike and sample are carried in different solid materials. Indeed even with the flux, we remain concerned by this possibility. Therefore as described below we undertook experiments to assess the degree of spike-sample equilibration.

Once the cell has been prepared, it is loaded into a vacuum chamber, evacuated to high vacuum, and baked at ∼100 °C to remove adsorbed gases. Higher bake-out temperatures are desirable to reduce atmospheric argon levels, but run the risk of Ar loss from sample, spike, or both.

After a few hours of bake-out the vacuum chamber is isolated from the pump, and the sample heated to a temperature at which the sample is readily digested by the molten flux, ∼965 °C. This causes argon to be degassed into the chamber from both the sample and the spike glass. When degassing is complete the heating is terminated and the argon purified and measured by mass spectrometry. In this step, the objective is to achieve complete extraction of argon with minimal volatilization loss of potassium. In the next step, the crucible is heated to a higher temperature (∼1030 °C) to intentionally volatilize potassium from the melt. The volatilized potassium is also analyzed by mass spectrometry. These two isotope dilution measurements are sufficient to define the sample K–Ar age (Eq. (10)).

At this stage of method development we do not have a single mass spectrometer configured to make both argon and potassium measurements, so we combined two separate instruments to demonstrate the concept and to evaluate some of the assumptions that underlie the technique. In the first stage of our current method, the sample is outgassed in the Knudsen cell and argon analyzed on a conventional noble gas mass spectrometer. Next the cell is retrieved from the vacuum furnace and transferred (without additional processing) into a Knudsen-effusion mass spectrometer (Drowart et al., 2005) for potassium analysis. We discuss ways to combine these two steps in a single instrument in the final section.

There are several fundamental requirements for this methodology to accurately yield the $^{40}Ar^*/^{40}K$ ratio from which the sample's K–Ar age is computed. The purpose of the experimental work described in the next section is to evaluate the following assumptions: (1) argon can be quantitatively degassed from spike and sample at a temperature low enough that neither bulk potassium loss nor extensive mass fractionation preclude accurate potassium isotope ratio determination; (2) $^{39}K/^{41}K$ ratios can be accurately measured by Knudsen effusion mass spectrometry on the residue remaining after argon extraction, even in the presence of competing effusing species of lithium and boron from the flux; (3) equilibration between spike and sample isotopes of both argon and potassium is adequate to accurately characterize the isotopic composition of the system. As a final test to see whether the method can yield accurate K–Ar ages and to evaluate likely sources of uncertainty, we determined the double isotope dilution K–Ar age of a basalt of independently known age.

3. METHODS

3.1. Preparation and characterization of the spike glass

The spike glass must be a homogeneous solid phase isotopically enriched in both ^{39}Ar and ^{41}K, in known relative proportions. The glass must retain Ar during handling and bake-out, and must readily dissolve in the lithium borate flux. For practical reasons we chose an alkali-rich aluminosilicate glass composition. By neutron irradiation we were able to ensure a homogenous $^{39}Ar/^{39}K$ ratio in the glass, and as long as the potassium is isotopically uniform, this ensures a uniform $^{39}Ar/^{41}K$ ratio.
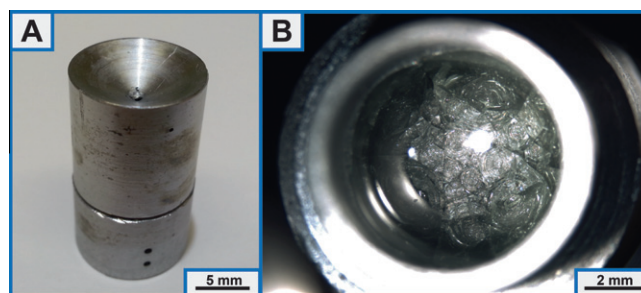
Fig. 1. (A) Close-up of the Knudsen cell showing the effusion orifice; (B) image of Knudsen Cell JAC1 following analysis of flux, spike glass and basalt sample for noble gases. The flux melted to form a glass, which shows prominent conchoidal fractures (possibly related to cooling rate). Neither basalt nor spike glass fragments were observed in or on this glass following analysis.

3.1.1. Synthesis

The preparation method of the spike glass was dictated by the availability of ^{41}K only in the form of KCl; the following synthesis method successfully incorporates the ^{41}K into a silicate glass while effectively removing the chlorine, which would transmute to undesirable isotopes of argon during neutron irradiation. The spike batch described below is the one used in the pilot measurements described here. Refinements to eliminate some contaminants are also described.

Albite glass was taken from a large batch prepared by Corning Glass Works. This material is very close to albite stoichiometry ($NaAlSi_3O_8$) and was previously thought to be devoid of contamination by any minor elements. 75 mg of crushed albite glass were placed in an open $Pd_{76}Au_{24}$ alloy cup (3 mm inner diameter, 15 mm high). To this was added 25 mg of fine grains of ^{41}KCl (99% isotopic purity) obtained from the isotope synthesis facility at Oak Ridge National Laboratory. To minimize losses of the isotopically enriched material and contamination of the laboratory, the ingredients were not mixed or ground at this stage. The furnace was prepared at 1150 °C (above the liquidus of albite) with a streaming gas-mix of H_2 and CO_2 that yielded an fO_2 one half of a log unit above the iron–wüstite buffer (IW + 0.5), measured with an yttria-stabilized zirconia oxygen sensor (see Balta et al. (2011) for gas-mixing and fO_2 measurement practices in this laboratory). This oxygen fugacity yields the maximum available fH_2O in the gas stream, approximately 0.6 bar. Under these conditions the volatilization of chlorine from the sample occurs by the reaction

$$2KCl(melt) + H_2O(g) = K_2O(melt) + 2HCl(g),$$
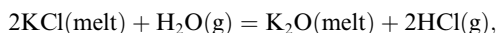
retaining as much as possible of the ^{41}K in the melt while degassing most of the chlorine. The sample was held at these conditions for 48 h and quenched by withdrawing the sample from the furnace and plunging it into cold water. Despite these precautions we still lost about 50% of the starting potassium content during synthesis.

In developing this method we undertook initial experiments with isotopically natural KCl; this produced a glass of similar bulk composition to the spike glass. We used this "natural-K glass" in some of the experiments described below.

3.1.2. FE-SEM and electron microprobe analysis

The result of this preparation is a glass bead with a milky grey appearance on the surface. The bead was broken and a chip of about 1 mm^3 was mounted in epoxy, polished, and carbon-coated. Upon examination with a field-emission scanning electron microscope at high magnification, the milkiness was found to result from a fine dispersion of Au–Pd–Sb alloy nanoparticles near the outer surface of the bead. Au and Pd are not an issue for the subsequent processing of this spike sample. However the Sb contamination proved problematic, as stable ^{123}Sb was transmuted during neutron irradiation into the short-lived isotope ^{124}Sb ($t_{1/2} = 60$ days), which in turn required sequestration of the spike glass for some months before further use, and dictated using the smallest possible amount of spike in the analyses to avoid radioactive contamination of our mass spectrometers. The bulk sample composition was estimated by energy-dispersive X-ray analysis while rastering the beam over a 100×100 μm area including both the region affected by the Sb contamination and the clear interior of the bead. Bulk Sb content was ~0.2 wt%.

The glass composition was then quantitatively analyzed on the Caltech JEOL JXA-8200 microprobe, operating at 15 kV accelerating potential with a 10 nA beam defocused to a 10 μm spot in order to minimize alkali mobilization. Standards were albite (for Na, Si, and Al), orthoclase (for K), anorthite (for Ca), forsterite (for Mg), fayalite (for Fe), and sodalite (for Cl). Ca, Mg, and Fe were below detection limits. The average and standard deviation of 22 analysis spots on the glass chip are given in Table 2; these replicate analyses pass a statistical homogeneity test at 95% confidence. The sample contains 7.01 ± 0.02 wt% K_2O (here and elsewhere stated uncertainties are at the 1σ level) and ⩽0.2 wt% Cl. Note that for the K_2O weight percent we have taken into account the unusual isotopic composition of the spike K in the glass.

After searching through possible sources of Sb contamination ($Pd_{76}Au_{24}$ capsule stock, ^{41}KCl supply, albite glass, alumina furnace tubes, mortar and pestle, etc.), it was traced to the Corning albite glass. Presumably Sb_2O_3 was used as a firing agent to suppress bubble formation in the glass. As described in Appendix A, we synthesized a second batch of spike glass free of Sb, however the work reported here used the contaminated material prepared in the first batch.

An ~1 mg chip of this glass was dissolved in 2:1 concentrated HF–HNO_3, taken to dryness, and redissolved in 5% concentrated HNO_3 in Milli-Q ultraclean water. The resulting solution, and blank and isotopically normal potassium

Table 2
Analytical data on spike glass.

Bulk	SiO_2 (wt%)	±	Al_2O_3 (wt%)	±	Na_2O (wt%)	±	K_2O (wt%)	±
	68.3	0.04	18.4	0.3	6.6	0.1	7.01	0.02
Argon	^{39}Ar (pmol/g)	±	$^{40}Ar/^{39}Ar$					
	1.989	0.05	<5					
Potassium	^{41}K (mmol/g)	±	$^{39}K/^{41}K$	±				
	1.369	0.004	0.0390	0.0006				
Combined	$^{39}Ar/^{41}K$ ($\times 10^{-9}$)	±						
	1.453	0.037						

standard solutions prepared in the same way, were analyzed for K isotopes on a Thermo-X series ICPMS fitted with a H_2 collision cell. Blank and fractionation corrected K isotope ratio results are shown in Table 2, indicating that 96.2% of the K in the glass is ^{41}K. This is slightly lower than the nominal purity of the ^{41}K-enriched KCl, probably due to contamination with natural potassium during synthesis. Coupled with the electron probe K_2O determination, these data imply a ^{41}K concentration of 1.369 ± 0.004 mmol ^{41}K/g, and $r_{spk} = 0.039$. We assume that the potassium isotopic composition is homogeneous within the glass.

After 40 h of irradiation in the cadmium-lined in-core irradiation tube (CLICIT) in the TRIGA reactor at Oregon State University, the spike glass was found to be unexpectedly radioactive. Several weeks after the irradiation >90% of the activity was found to derive from ^{124}Sb. The spike glass was allowed to cool for several more months before further processing; at this stage the radioactivity was sufficiently low that exposing our analytical equipment to ∼500 μg quantities of the material was deemed acceptable. (Ideally, the experiment would have used a few mg of spike glass to permit greater precision in ^{39}Ar determinations, see below.)

Five aliquots of spike glass weighing between 0.2 and 0.6 mg were fused in a double-walled resistance furnace at ∼1500 °C. The evolved ^{39}Ar was purified of contaminating species and yielded ∼1000 cps on the electron multiplier spur of a MAP 215-50 mass spectrometer. About 15 cps of mass 39 was consistently measured on furnace blanks, presumably from an unresolved isobaric contaminant. This amount was subtracted from the signal evolved from the spike glass. A standard consisting of ∼2.7×10^{-12} mol of atmospheric argon was used to establish sensitivity, mass fractionation, and the faraday-multiplier cross calibration factor. The ^{39}Ar concentration was determined to be 1.989 ± 0.05 pmol/g (Table 2). Based on documented neutron flux gradients in materials analyzed in an identical fashion at the OSU reactor (Simon et al., 2009), and the observed homogeneity in K concentration of the glass (Table 2), this ^{39}Ar concentration should be homogenous to better than 1%. No other argon isotopes were detected above blank, and are not expected given the very small

amount of spike glass analyzed. Our data place an upper limit on the glass $^{40}Ar/^{39}Ar$ ratio (R_{spk}) of 5; it could be much lower. Note that reactor produced ^{40}Ar from neutron capture on ^{40}K is likely to be very small in our glass because we are using highly ^{41}K-enriched potassium (and used Cd shielding during irradiation), so we expect very little neutron-produced ^{40}Ar. However, we cannot rule out the possibility of atmospheric ^{40}Ar contamination. Even at the upper limit of $R_{spk} \sim 5$, the amount of ^{40}Ar coming from the spike during sample analyses is negligible.

Taken together, we find the double-isotope spike ratio $(^{39}Ar/^{41}K)_{spk} = 1.45 \times 10^{-9}$ with an estimated uncertainty of 2.5%.

3.2. Basalt sample and flux

To test the method we chose a basalt with a typical potassium concentration (about 0.8 wt% K_2O) and a well-determined age. To this end we obtained whole rock crushate of sample 42a/01 from the Viluy traps (Eastern Siberia; Courtillot et al. 2010). This sample, drilled from a dolerite dike, is a tholeiitic to sub-alkaline basalt composed of plagioclase, clinopyroxene, and minor olivine. Analyses of plagioclase fractions yielded concordant ages of 351.4 ± 5 and 354.3 ± 5 Ma by K–Ar and $^{40}Ar/^{39}Ar$ (integrated) methods, respectively. For our experiments we used bulk crushate in the 100–500 μm size fraction.

For the flux we chose a 50:50 mixture of lithium metaborate:lithium tetraborate (ultrapure grade, obtained from Spex Certiprep). This particular proportion was chosen for its remarkable ability to digest a wide range of mineral and rock compositions, including silicates, sulfates, carbonates, and oxides.

3.3. Noble gas mass spectrometry

In this step the Knudsen cell was loaded with 150 mg of flux, introduced into a double-walled vacuum furnace, evacuated to <10^{-7} torr with a turbomolecular pump, and heated to ∼1000 °C. In an initial attempt the flux was heated to temperature in about 10 min, causing violent

bubbling and climbing of the flux up the walls of the Knudsen cell. Heating the sample to temperature over ~45 min eliminated this problem. After 30 min of degassing at ~1000 °C the cell was cooled and removed from the furnace. For the analysis of the sample (referred to as analysis JAC-1) 10 mg of the Viluy basalt sample and 179 μg of the spike glass were placed in the bottom of the cell, directly on top of the lithium borate glass, returned to the furnace, and evacuated and gently baked (~100 °C) overnight to liberate adsorbed Ar.

For argon extraction and analysis the vacuum chamber was isolated from the pump and the heating process repeated. JAC-1 was degassed in two steps, at ~400 °C to drive off atmospheric contamination, and again to 965 °C to melt the flux and completely degas the sample. In both cases we used a 45 min heating ramp with 30 min at the setpoint. After degassing, the sample was allowed to cool to <300 °C before introducing the gas into the processing line. Argon was purified and analyzed as described for the spike glass except ^{40}Ar and ^{36}Ar were measured on a Faraday collector, while ^{38}Ar and ^{39}Ar were measured on the electron multiplier. JAC-1 was heated a second time to 965 °C to assess completeness of extraction of spike and radiogenic argon.

In this design it is not possible to degas the furnace prior to heating the sample; this contributes to an unusually large argon blank as the furnace is first heated. For example, furnace blanks that consisted only of flux (no sample) were about ~0.85 pmol of ^{40}Ar with an air-like composition on the first heating to 965 °C, but in subsequent heating steps this blank dropped substantially. We assumed a value of 0.85 pmol for our blank corrections. Because the blank has an air-like composition, uncertainty in the blank amount does not affect the final computation of $^{40}Ar^*$.

3.4. Knudsen effusion mass spectrometry (KEMS)

KEMS is a well-established technique for studying inorganic vapors (Drowart and Goldfinger, 1967; Drowart et al., 2005) and is a logical choice for measurement of the potassium isotope ratio evolved from our sample cell. After argon extraction, the cell was shipped to the NASA Glenn Research Center, where it was placed in a typical Knudsen cell heating assembly (Drowart and Goldfinger, 1967; Copland and Jacobson, 2010). During heating of the cell by a tantalum 'hair-pin' shaped resistance heater, vapor is liberated from the fluxed mixture into the cell. A small portion of that vapor effuses through the orifice in the lid and passes through the ion source of the mass spectrometer. Temperature was measured with a Type R thermocouple strapped to the Knudsen cell and calibrated with the melting point of silver. A magnetic sector mass spectrometer (modified Nuclide/MAAS 12-90-HT), an electron impact ionization source, and a 20 dynode electron multiplier with ion counting were used for these measurements (Copland and Jacobson, 2010). This configuration minimizes mass discrimination (Roboz, 1968), making the system ideal for isotope ratio measurements. The instrument is configured so that the molecular beam, ionizing electrons, and resultant ion beam are all mutually perpen-

dicular. For these measurements we used an ion source electron energy of 60 eV. This rather high ionizing electron energy assured fragmentation of all K-containing components in the vapor, so that the potassium signal was representative of the entire sample. The resolution as defined by the source exit slit and multiplier entrance slit is about 1100, which allows separation of the inorganic peaks from any background hydrocarbons. In addition, oil-free pumping was utilized through magnetically levitated turbomolecular pumps on the Knudsen cell chamber and ion source and ion pumps on the flight tube and detector.

Several different materials were analyzed by KEMS. The first set of experiments were designed to establish how potassium behaves when volatilized from mixtures of flux and basalt and flux and natural-K glass (the spike glass analog). The second experiment was designed to assess mass fractionation during evolution of potassium from a mixture of natural-K glass and flux. The third experiment was the analysis of JAC-1, the basalt + spike glass + flux mixture.

4. RESULTS

4.1. Argon

Argon results obtained on JAC-1 are shown in Table 3. About 7% of the total ^{39}Ar was released in the first heating step (~400 °C), a quantity easily distinguished above blank levels for this isotope. In contrast the $^{40}Ar/^{36}Ar$ ratio of 306 in the 400 °C step was only slightly elevated compared to the atmospheric ratio (299). A far higher $^{40}Ar/^{36}Ar$ ratio of 651 was obtained in the 965 °C step. These data imply that ~97% of the radiogenic argon was released in the high temperature step when the basalt was flux-melted. A repeat extraction at 965 °C released no additional ^{39}Ar or $^{40}Ar^*$, demonstrating the efficacy of flux melting in liberating argon from both the basalt and the spike glass.

These results suggest that our low temperature "cleanup" step was done at slightly too high a temperature – we cannot exclude this step from the computation of the total yields from JAC-1. Thus we combined data from the two steps to obtain $^{40}Ar/^{39}Ar$ and $^{36}Ar/^{39}Ar$ ratios of 44,300 and 102, respectively. This corresponds to a bulk $^{40}Ar/^{36}Ar$ ratio of 432 and a radiogenic argon fraction of 0.31.

4.2. Potassium

The evolution of the $^{39}K^+$ signal with temperature during the KEMS experiments performed on basalt and on the natural-K glass, both with flux, are shown in Fig. 2. For these runs the cell was heated at a rate of 3 °C/min. For both runs the potassium signal below ~840 °C is quite low, consistent with little solid-phase release from the starting materials. However, as the flux is heated above the melting point of lithium metaborate (845 °C), the ion intensity rises rapidly. The transition at this temperature is consistent with the onset of dissolution of the sample into the molten flux, while the exponential increase at higher temperatures likely arises from increasing vapor pressure of K over the melt.

The release pattern for the two specimens as a function of temperature is broadly similar, with the only notable

Table 3
Analytical data on JAC-1 (Viluy 42a/01 basalt).

Experiment	$^{39}K/^{41}K$	±	$^{40}Ar/^{39}Ar$	±	$^{36}Ar/^{39}Ar$	±	K–Ar age (Ma)	±
JAC-1	4.71	0.07	44300	740	102	2	351	19

difference being how steeply the $^{39}K^+$ signal increases above ~940 °C, which is more than two hours into the experiment. At this temperature/time it seems likely that both basalt and natural-K glass are entirely dissolved in the flux. Thus the difference in behavior above this temperature suggests either that the basaltic melt is approaching exhaustion of its potassium at a more rapid rate than the natural-K glass (consistent with its nearly order-of-magnitude lower K content), or the vapor pressure of potassium over the lithium borate liquid depends on the liquid composition. Regardless of why this difference exists, the general similarity in behavior between these two systems suggests that isotopic homogenization between the spike and sample potassium will occur in the melt and/or the Knudsen cell, such that, in the absence of mass fractionation, the evolved vapor will be an accurate representation of the isotopic composition of the mixture.

Fig. 3 shows the evolution of the $^{39}K/^{41}K$ ratio during heating of a second aliquot of natural-K glass + flux mixture. This mixture was heated to 980, 1030 and 1065 °C, and at each temperature the $^{39}K/^{41}K$ ratio was measured for 30 min. At ~980 °C the ratio is somewhat scattered, presumably because the ion intensities are fairly small (<40 cps on ^{41}K). Ratios at the two higher temperatures are more consistent. When plotted against the cumulative fraction of ^{39}K measured in the experiment, there is a slight decreasing trend in the $^{39}K/^{41}K$ ratio. In addition, the yield of ^{39}K per unit time decreases at the highest temperature. Both of these observations are consistent with depletion

of potassium from the charge, with associated fractionation of the residue towards a heavier isotopic composition. Importantly, our measurement is an integral of all of the potassium analyzed rather than a point measurement at a given time or temperature. As shown in Table 3 and by the horizontal line in Fig. 3, this run yielded an integrated $^{39}K/^{41}K$ ratio of 13.85 ± 0.21, in excellent agreement with the natural $^{39}K/^{41}K$ ratio of 13.86. This observation indicates that the integral potassium isotope ratios obtained from KEMS are not substantially fractionated from the starting composition.

These data can also be used to set an upper limit on the fraction of potassium evolved from JAC-1 while heating to 965 °C during the argon extraction. If we assume that all of the potassium was effused during the KEMS run, then the data in Fig. 3 imply that at 980 °C, potassium is being lost from the Knudsen cell at a rate of 1%/min. Thus in our 30 min argon degassing of JAC-1 we will have lost no more than 30% of the total potassium. This is a strong upper limit because (a) the argon degassing occurred at 965 °C, not 980 °C, and the potassium release curve is quite steep in this temperature range (Fig. 2), and (b) we did not completely degas potassium from the sample in Fig. 3, thus the loss rate is an overestimate. The importance of this conclusion is that it implies that the loss of potassium during the argon degassing step does not remove enough potassium to threaten our ability to measure the isotope ratio by KEMS, nor does it isotopically fractionate the residue to a significant degree.
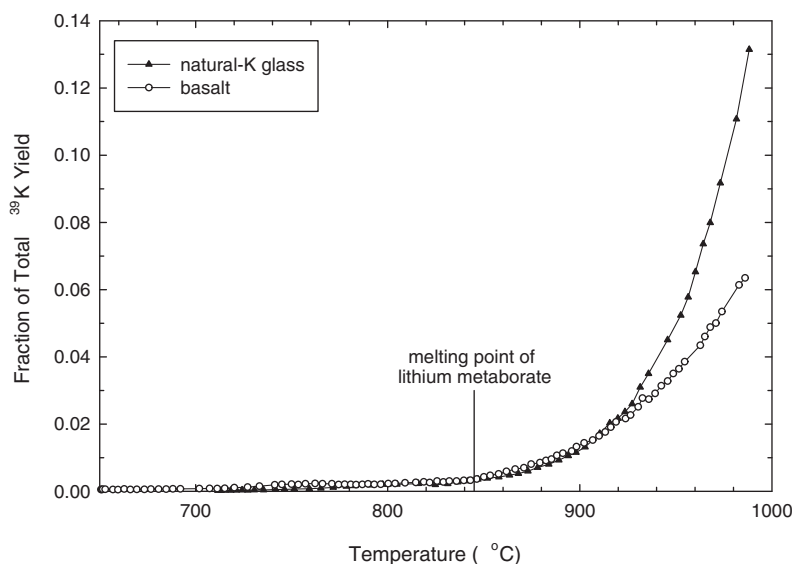

Fig. 2. $^{39}K^+$ evolution by KEMS. Samples are mixtures of lithium borate flux with basalt and with the natural-K glass; the sample/flux mass ratio was 0.25. The $^{39}K^+$ signal in each step has been normalized to the total yield obtained from each entire run. Note the change in K release behavior at 845 °C, the melting point of lithium metaborate.
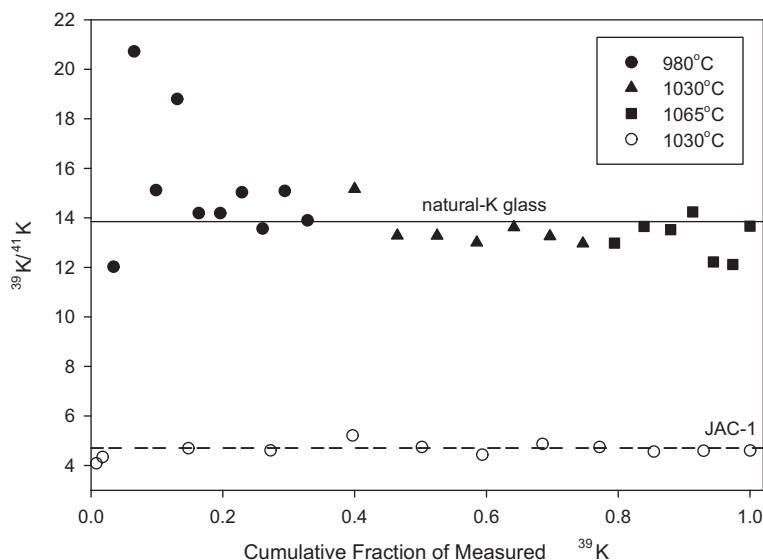
Fig. 3. Potassium isotope ratio evolution from a mixture of the normal K-glass and lithium borate flux and from JAC-1. The *x*-axis is a measure of the total amount of ^{39}K degassed from the Knudsen cell. For the natural-K glass the cell was held at each of the three indicated temperatures for 30 min. For JAC-1 the cell was held at a constant temperature of ~1030° C for 1 h. The horizontal lines are the integrated ^{39}K/^{41}K ratio from the sample. For the natural-K glass the integrated ratio is the same within error as the known ratio for natural K.

The final KEMS experiment was the analysis of JAC-1, the mixture of flux, basalt, and spike glass previously analyzed for argon. This mixture was analyzed for ^{39}K/^{41}K ratio at 1040 °C for about one hour. During this time there was no noticeable change in isotopic composition. As indicated in Table 3, the sample yielded an integrated ^{39}K/^{41}K ratio of 4.71 ± 0.07.

4.3. Age computation

These data provide the three quantities required to compute a K–Ar age for JAC-1 from Eq. (10): $R_m = 44,300 \pm 740$, $(^{36}Ar/^{39}Ar)_m = 102 \pm 1.8$, and $r_m = 4.71 \pm 0.07$. Combined with the spike characteristics listed in Table 2, the resulting K–Ar age is 351 ± 19 Ma. This number compares favorably to the published ages for Viluy 42a/01 of 351.4 ± 5 and 354.3 ± 5 Ma by K–Ar and $^{40}Ar/^{39}Ar$, respectively (Courtillot et al., 2010).

5. DISCUSSION AND CONCLUSIONS

These experiments support the assumptions and procedures necessary to accurately determine the K–Ar age using the double isotope dilution method. In particular, heating to 965 °C for 30 min is adequate to quantitatively degas argon from both the spike glass and the basalt. This temperature and time cause only modest potassium loss from the Knudsen cell, and as a result the potential for potassium isotopic fractionation is limited. Experiments on basalt and spike glass measured independently, as well as on the Viluy basalt sample, strongly support equilibration of spike and sample potassium isotopes prior to the KEMS isotopic ratio measurement. As a result, the measured isotope ratio is an accurate measurement of the potassium composition of the bulk system. No practical difficulties were encoun-

tered for measuring potassium evolved from the Knudsen cell. Although lithium borate was presumably also volatilized, it does not interfere with the potassium measurement.

The measured age on the Viluy basalt is well within error of previous measurements of the age of this sample. The estimated analytical uncertainty of the current implementation of this technique is ~6%. This is somewhat poorer than what one might expect from two isotope dilution measurements, which in general are expected to yield precisions at least twice as good. This warrants an evaluation of the sources of uncertainty in our methodology. Although we have limited experimental evidence for the individual uncertainties we adopted, several observations are relevant. The uncertainty on the $^{39}Ar/^{41}$K of the spike contributes only ~10% of the total uncertainty. This makes sense because the spike glass composition was determined by averaging of multiple analyses. Indeed, in principle this source of uncertainty can be made arbitrarily small by replication. Of the remaining uncertainty ~65% comes from the argon measurements and the remainder from the potassium isotope ratio. The relatively large argon uncertainty arises from two obvious factors: the very small ^{39}Ar beam and the large correction for atmospheric argon. The ^{39}Ar signal in our experiment was far lower than optimal owing to the small amount of spike glass used, a consequence of our effort to minimize the amount of radioactive antimony contaminant potentially released into our mass spectrometers. This complication motivated the synthesis of an antimony-free spike for future use (see Appendix A), which will allow larger spike glass masses and hence better argon isotope ratio precision. The large atmospheric argon correction can be reduced by designing a system that allows degassing of the heater prior to the accumulation of sample argon. Solutions to both of these problems are straightforward and should allow the method to approach an age pre-

cision significantly better than 5%. Such improved precision is necessary to identify likely smaller sources of uncertainty and to assess the ultimate precision of the method.

The double-isotope dilution method has the potential to yield K–Ar measurements using relatively simple and proven analytical techniques that are available for space-flight application. For example, the SAM instrument in the payload of the Mars Science Laboratory includes both an oven capable of heating sample material to 1100 °C, as well as a quadrupole mass spectrometer with a pulse-counting electron multiplier with sensitivity similar to the mass spectrometers used in this pilot study (Mahaffy et al., 2012).

The final step required to implement this method for space flight or even terrestrial laboratory use is to combine the K and Ar measurements into a single analytical instrument. Both of the mass spectrometers we used produced ions in the same way: by electron impact ionization. The mass spectrometers were also nearly identical. Thus a single mass spectrometer with an appropriate ion source can make the requisite measurements provided that argon and potassium can be delivered to the ion source automatically and in sequence. One logical route to this objective is to design a low argon blank vacuum chamber (all metal and bake-able chamber and valves, minimal inclusion of ancillary equipment in the chamber) that houses both a cross-beam electron impact ion source and mass spectrometer. In such a system the sample would be heated under static vacuum, allowing effusing potassium to be directed through the ion source and analyzed by the mass spectrometer while argon gas is accumulating. By using an appropriately low electron energy in the ion source (say 10 eV) it is possible to very efficiently ionize potassium without ionizing argon at all (based on electron impact ionization cross sections, Wetzel et al., 1987). This low eV level precludes simultaneous detection of both potassium and argon isobars, and has the ancillary benefit of preventing ionization of hydrocarbons that might interfere, especially on mass 41 ($C_3H_5^+$). Once sufficient potassium isotope data is obtained, the heater can be turned off and the argon gas cleaned up by exposure to chemical getters. The ion source would then be tuned to an electron energy at which argon is ionized, and its isotope ratio measured. This sequence has the added virtue that only one heating step is required, reducing the overall power requirement for the analysis.

It is important to note that a K–Ar age is equivalent to the formation age of a sample only when the sample has remained a closed system for parent and daughter and when it is free of ^{40}Ar from sources other than ^{40}K decay and atmospheric contamination. Phenomena such as slow-cooling as well as reheating associated with burial, nearby volcanism, or impacts may induce argon loss that will cause the K–Ar age to underestimate the sample formation age. Similarly, excess ^{40}Ar may cause erroneously high estimates of ^{40}Ar* and hence K–Ar ages that are older than the sample formation age. The latter is thought by some authors to be especially problematic in the case of martian basalts. In particular, an excess ^{40}Ar component in many shergottite meteorites causes ^{40}Ar/^{39}Ar ages to exceed ages obtained by other methods. For example, in the case of the Zagami shergottite, Bogard and Park (2008) obtained a ^{40}Ar/^{39}Ar

age of about 220 Ma, while other techniques yield ages of ∼170 Ma (Nyquist et al., 2001; Borg et al., 2005). A mantle ^{40}Ar component of approximately equal concentration may be present in all shergottite meteorites (Bogard and Garrison, 1999; Bogard and Park, 2008; Bogard, 2009). This led Bogard (2009) to suggest the necessity of an isochron method with a perhaps prohibitively large number of aliquot analyses for accurate in situ K–Ar dating of martian basalts. While excess argon is likely present in all basalts (martian and otherwise), the consequences for in situ dating, at least at the excess ^{40}Ar levels that have been documented thus far, are not as substantial as this conclusion implies. For example, the same amount of excess ^{40}Ar reported in the shergottites (Bogard and Park, 2008; Bogard, 2009) in a rock with the same K content as Zagami but a formation of 3.5 Ga would yield a K–Ar age of 3.54 Ga, certainly too small a difference to be considered consequential. While the impact of excess ^{40}Ar becomes increasingly great with decreasing sample age, it is not obvious that even a 50 Ma error on a sample as young as the shergottites (∼200 Ma) would preclude useful interpretation. Nevertheless both excess argon and argon loss are factors that should be carefully evaluated when considering in situ K–Ar dating of any particular planetary surface.

Although analyses of additional samples are required, the double isotope dilution technique described here appears capable of providing K–Ar ages with a routine precision of better than 5%. This precision is dictated by the ability to measure isotope ratios, a well understood process for both potassium and argon. A maximum temperature of just 1030 °C is required, and no mass estimate is necessary. Existing flight-qualified hardware can perform the necessary heating and probably the mass spectrometry. The remaining challenge is to develop the physical apparatus that allows sequential ionization of potassium and argon evolved from a sample to be dated.

APPENDIX A

To eliminate the radioactive Sb in the first batch of the isotope dilution spike, a new batch of spike was prepared in a multistep procedure. First, clean albite glass was synthesized from alpha Aesar Puratronic SiO_2, Al_2O_3, and Na_2CO_3 by decarbonating at 500 °C followed by melting at 1150 °C. This material was ground and mixed in a 3:1 weight ratio with ^{41}KCl. The mixture was fired in an open Pt (not $Pd_{76}Au_{24}$) cup for 90 h at IW + 0.5, fH$_2$O = 0.6 bar and 1150 °C, quenched, reground, and fired again for an

additional 48 h under the same conditions. Although this product contained no Sb and very little Cl, it retained enough K_2O to move into the liquidus field of leucite (KAl_2SiO_6). Hence it was melted again, this time in a sealed Pt capsule to prevent volatilization of K, at 1350 °C for four hours and finally quenched to obtain a clean, homogenous glass free of any elements besides O, Na, Al, Si, Cl, and K at electron microprobe detection limits.

Three chips of this glass product were also analyzed on the Caltech microprobe, using the same analytical conditions and standardization procedures described above. The sample contains a reported 9.1 ± 0.2 wt% K_2O and 0.23 ± 0.03 Cl wt%. It contains neither dispersed antimony nor the Au-Pd-Sb droplets seen in the first spike glass. As of the time of writing, this glass has not yet been neutron-irradiated; the experiment described in the main text makes use of the initial Sb-contaminated spike glass.

REFERENCES

Anderson F., Nowicki K., Hamilton V. and Whitaker T. (2012) Portable geochronology with LDRIMS: learning to date meteorites like Zagami with the Boulder Creek granite. *Lunar Planet. Sci. 43*. Lunar Planet. Inst., Houston. #2844 (abstr.).

Balta J. B., Beckett J. R. and Asimow P. D. (2011) Thermodynamic properties of alloys of gold-74/palladium-26 with variable amounts of iron and the use of Au–Pd–Fe alloys as containers for experimental petrology. *Am. Mineral.* **96**, 1467–1474.

Bell, III, J. F. (2008) *The Martian Surface: Composition, Mineralogy and Physical Properties*. The Cambridge University Press, Cambridge, 652pp.

Bibring J. P., Langevin Y., Mustard J. F., Poulet F., Arvidson R., Gendrin A., Gondet B., Mangold N., Pinet P. and Forget F., et al. (2006) Global mineralogical and aqueous mars history derived from OMEGA/Mars express data. *Science* **312**, 400–404.

Bogard D. D. (2009) K–Ar dating of rocks on Mars: requirements from Martian meteorite analyses and isochron modeling. *Meteorit. Planet. Sci.* **44**, 3–14.

Bogard D. D. and Garrison D. L. H. (1999) Argon-39-argon-40 "ages" and trapped argon in Martian shergottites, Chassigny, and Allan Hills 84001. *Meteorit. Planet. Sci.* **34**, 451–473.

Bogard D. D. and Park J. (2008) Ar-39–Ar-40 dating of the Zagami Martian shergottite and implications for magma origin of excess Ar-40. *Meteorit. Planet. Sci.* **43**, 1113–1126.

Borg L. E., Edmunson J. E. and Asmerom Y. (2005) Constraints on the U–Pb isotopic systematics of Mars inferred from a combined U–Pb, Rb–Sr, and Sm–Nd isotopic study of the Martian meteorite Zagami. *Geochim. Cosmochim. Acta* **69**, 5819–5830.

Carr M. H. (1996) *Water on Mars*. Oxford University Press, New York, 229pp.

Carr M. H. and Head, III, J. W. (2010) Geologic history of Mars. *Earth Planet. Sci. Lett.* **294**, 185–203.

Cho Y., Miura Y. N. and Sugita S. (2012) Development of a laser ablation isochron K–Ar dating instrument for landing planetary missions. *International Workshop on Instrumentation for Planetary Missions*. Goddard Space Flight Center, Maryland, USA. #1093 (abstr.).

Cohen B. A. (2012) Development of the potassium-argon laser experiment (KARLE) instrument for in situ geochronology. *43rd Lunar Planet. Sci. Conf.* Houston. #1267 (abstr.).

Copland E. H. and Jacobson N. S. (2010) *Measuring Thermodynamic Properties of Metals and Alloys with Knudsen Effusion Mass Spectrometry*. NASA/TP—2010-216795.

Courtillot V., Kravchinsky V. A., Quidelleur X., Renne P. R. and Gladkochub D. P. (2010) Preliminary dating of the Viluy traps (Eastern Siberia): eruption at the time of Late Devonian extinction events? *Earth Planet. Sci. Lett.* **300**, 239–245.

Drowart J., Chatillon C., Hastie J. and Bonnell D. (2005) High-temperature mass spectrometry: instrumental techniques, ionization cross-sections, pressure measurements, and thermodynamic data – (IUPAC technical report). *Pure Appl. Chem.* **77**, 683–737.

Drowart J. and Goldfinger P. (1967) Investigation of inorganic systems at high temperature by mass spectrometry. *Angew. Chem. Int. Ed.* **6**, 581–648.

Ehlmann B. L., Mustard J. F., Murchie S. L., Bibring J. P., Meunier A., Fraeman A. A. and Langevin Y. (2011) Subsurface water and clay mineral formation during the early history of Mars. *Nature* **479**, 53–60.

Gellert R., Rieder R., Bruckner J., Clark B. C., Dreibus G., Klingelhofer G., Lugmair G., Ming D. W., Wanke H., Yen A., Zipfel J. and Squyres S. W. (2006) Alpha particle X-ray spectrometer (APXS): results from Gusev crater and calibration report. *J. Geophys. Res. Planets* **111**. http://dx.doi.org/10.1029/2005.

Hartmann W. K. and Neukum G. (2001) Cratering chronology and the evolution of Mars. *Space Sci. Rev.* **96**, 165–194.

Hauber E., Broz P., Jagert F., Jodlowski P. and Platz T. (2011) Very recent and wide-spread basaltic volcanism on Mars. *Geophys. Res. Lett.* **38**, 5. http://dx.doi.org/10.1029/2011.

Humayun M. and Clayton R. N. (1995) Potassium isotope cosmochemistry – genetic implications of volatile element depletion. *Geochim. Cosmochim. Acta* **59**, 2131–2148.

Kieffer H. H., Jakosky B. M., Snyder C. W. and Matthews M. S. (1992) *Mars*. The University of Arizona Press, Tucson, 1498pp.

Mahaffy P. R., Webster C. R., Cabane M., Conrad P. G., Coll P., Atreya S. K., Arvey R., Barciniak M., Benna M., Bleacher L., Brinckerhoff W. B., Eigenbrode J. L., Carignan D., Cascia M., Chalmers R. A., Dworkin J. P., Errigo T., Everson P., Franz H., Farley R., Feng S., Frazier G., Freissinet C., Glavin D. P., Harpold D. N., Hawk D., Holmes V., Johnson C. S., Jones A., Jordan P., Kellogg J., Lewis J., Lyness E., Malespin C. A., Martin D. K., Maurer J., McAdam A. C., McLennan D., Nolan T. J., Noriega M., Pavlov A. A., Prats B., Raaen E., Sheinman O., Sheppard D., Smith J., Stern J. C., Tan F., Trainer M., Ming D. W., Morris R. V., Jones J., Gundersen C., Steele A., Wray J., Botta O., Leshin L. A., Owen T., Battel S., Jakosky B. M., Manning H., Squyres S., Navarro-Gonzalez R., McKay C. P., Raulin F., Sternberg R., Buch A., Sorensen P., Kline-Schoder R., Coscia D., Szopa C., Teinturier S., Baffes C., Feldman J., Flesch G., Forouhar S., Garcia R., Keymeulen D., Woodward S., Block B. P., Arnett K., Miller R., Edmonson C., Gorevan S. and Mumm E. (2012) The sample analysis at Mars investigation and instrument suite. *Space Sci. Rev.* **170**, 401–478.

Maurice S., Wiens R. C., Saccoccio M., Barraclough B., Gasnault O., Forni O., Mangold N., Baratoux D., Bender S., Berger G., Bernardin J., Berthe M., Bridges N., Blaney D., Bouye M., Cais P., Clark B., Clegg S., Cousin A., Cremers D., Cros A., DeFlores L., Derycke C., Dingler B., Dromart G., Dubois B., Dupieux M., Durand E., d'Uston L., Fabre C., Faure B., Gaboriaud A., Gharsa T., Herkenhoff K., Kan E., Kirkland L., Kouach D., Lacour J. L., Langevin Y., Lasue J., Le Mouelic S., Lescure M., Lewin E., Limonadi D., Manhes G., Mauchien P., McKay C., Meslin P. Y., Michel Y., Miller E., Newsom H. E., Orttner G., Paillet A., Pares L., Parot Y., Perez R., Pinet P., Poitrasson F., Quertier B., Salle B., Sotin C., Sautter V., Seran H., Simmonds J. J., Sirven J. B., Stiglich R., Striebig N., Thocaven J. J., Toplis M. J. and Vaniman D. (2012) The

ChemCam instrument suite on the Mars Science Laboratory (MSL) Rover: science objectives and mast unit description. *Space Sci. Rev.* **170**, 95–166.

McDougall I. and Harrison T. M. (1988) *Geochronology and Thermochronology by the $^{40}Ar/^{39}Ar$ Method.* New York, Oxford, 274pp.

Murchie S. L., Mustard J. F., Ehlmann B. L., Milliken R. E., Bishop J. L., McKeown N. K., Dobrea E. Z. N., Seelos F. P., Buczkowski D. L., Wiseman S. M., Arvidson R. E., Wray J. J., Swayze G., Clark R. N., Marais D. J. D., McEwen A. S. and Bibring J. P. (2009) A synthesis of Martian aqueous mineralogy after 1 Mars year of observations from the Mars Reconnaissance Orbiter. *J. Geophys. Res. Planets* **114**, 30. http://dx.doi.org/10.1029/2009.

Nyquist L. E., Bogard D. D., Shih C.-Y., Greshake A., Stöffler D. and Eugster O. (2001) Ages and geologic histories of Martian meteorites. *Space Sci. Rev.* **96**, 105–164.

Renne P. R., Mundil R., Balco G., Min K. W. and Ludwig K. R. (2010) Joint determination of K-40 decay constants and Ar-40*/K-40 for the Fish Canyon sanidine standard, and improved accuracy for Ar-40/Ar-39 geochronology. *Geochim. Cosmochim. Acta* **74**, 5349–5367.

Roboz J. (1968) *Introduction to Mass Spectrometry; Instrumentation and Techniques.* Interscience, New York, 539pp.

Simon J. I., Vasquez J. A., Renne P. R., Schmitt A. K., Bacon C. R. and Reid M. R. (2009) Accessory mineral U–Th–Pb ages and $^{40}Ar/^{39}Ar$ eruption chronology, and their bearing on rhyolitic magma evolution in the Pleistocene Coso volcanic field, California. *Contrib. Miner. Petrol.* **158**, 421–446.

Swindle T. (2001) Could in-situ dating work on Mars? *Lunar Planet. Sci. 32.* Lunar Planet. Inst., Houston. #1492 (abstr.).

Swindle T., Bode R., Boynton W., Kring D., Williams M., Chutjian A., Darrach M., Cremers D., Wiens R. and Baldwin S. (2003) AGE (Argon Geochronology Experiment): an instrument for in situ geochronology on the surface of Mars. *Lunar Planet. Sci. 34.* Lunar Planet. Inst., Houston. #1488 (abstr.).

Talboys D. L., Barber S., Bridges J. C., Kelley S. P., Pullan D., Verchovsky A. B., Butcher G., Fazel A., Fraser G. W., Pillinger C. T., Sims M. R. and Wright I. P. (2009) In situ radiometric dating on Mars: investigation of the feasibility of K–Ar dating using flight-type mass and X-ray spectrometers. *Planet. Space Sci.* **57**, 1237–1245.

Wetzel R. C., Baiocchi F. A., Hayes T. R. and Freund R. S. (1987) Absolute cross-sections for electron impact ionization of the rare gas atoms by the fast neutral method. *Phys. Rev. A* **35**, 559–577.

Associate editor: Pete Burnard